The is a post-print. The accepted manuscript is available at:
Soutter, E.L., Kane, I.A., Hodgson, D.M. and Flint, S., 2021. The concavity of submarine canyon longitudinal profiles. *Journal of Geophysical Research: Earth Surface*, p.e2021JF006185.

Title: The concavity of submarine canyon longitudinal profiles

Authors: Euan L. Soutter[1], Ian A. Kane[1], David M. Hodgson[2], Stephen Flint[1],

Institutions: [1]Department of Earth and Environmental Sciences, University of Manchester, Manchester, M13 9PL, U.K.

[2]School of Earth and Environment, University of Leeds, Leeds, LS2 9JT, U.K.

Email: euan.soutter@manchester.ac.uk [Euan L. Soutter]

ORCID iD: https://orcid.org/0000-0001-8310-6414 [Euan L. Soutter]

KEY POINTS

- 377 submarine canyon longitudinal profiles and their concavities have been measured
- 66% of submarine canyons are concave (NCI < 0)
- Tectonics are the primary control on canyon concavity, with tectonically active margins hosting the least concave canyons

ABSTRACT

Submarine canyons incise continental shelves and slopes, and are important conduits for the transport of sediment, nutrients, organic carbon and pollutants from continents to oceans. Submarine canyons bear morphological similarities to subaerial valleys, such as their longitudinal (long) profiles. Long profiles record the interaction between erosion and uplift, making their shape, or concavity, a record of environmental and tectonic processes. The processes that govern concavity of subaerial valleys and rivers are well documented on a global scale, however, the processes that control submarine canyon concavity are less well constrained. We address this problem by utilizing existing geomorphological, tectonic and climatic datasets to measure the long profiles and quantify the concavities of 377 modern submarine canyons. Key results show that: (1) the dominant control on submarine canyon concavity is tectonics, with forearcs and tectonically active margins hosting the least concave-up profiles; (2) present-day canyon position affects canyon concavity, with river-associated canyons being less concave than canyons currently

dissociated from rivers on forearcs; (3) present-day onshore climate appears to have a more limited impact on submarine canyon concavity when compared to these factors. While significant local variation exists, these results indicate that tectonic processes are the dominant control on the concavity of submarine canyons on a global scale.

PLAIN LANGUAGE SUMMARY

Submarine canyons are primarily formed by erosion beneath dense underwater mixtures of sediment and water transported into the sea by rivers, and by submarine landslides. The record of erosion and deposition from these flows is preserved in the downstream, or longitudinal, profile of the submarine canyons they form. Submarine canyons are also affected by tectonic processes, such as seabed faults, which deform their longitudinal profiles. Since these tectonic and sedimentary processes vary globally, we wondered whether this variation is reflected in the longitudinal profiles of submarine canyons globally. We found out that in places where tectonic activity is great, such as western South America, submarine canyons tend to have more linear downstream profiles, while in places where tectonic activity is low, such as eastern North America, submarine canyons tend to have a more concave-up profile. We attribute this to; (1) deformation of canyon profiles by tectonic activity, and (2) high supplies of coarse-grained sediment on active margins. Submarine canyons therefore tend to have different shapes depending on where they are on the Earth's surface, which results from the different sedimentary and tectonic processes to which they are subject.

TEXT

1. Introduction

The relationship between elevation and downstream distance in subaerial valleys and channels, and submarine canyons and channels, is expressed in their longitudinal, or "long," profiles (e.g., Adams & Schlager, 2000; Covault et al., 2011; Dietrich et al., 2003; Georgiopoulou & Cartwright, 2013; Gerber et al., 2009; Huyghe et al., 2004; Mitchell, 2005; Pirmez et al., 2000; Whipple & Tucker, 1999; Yatsu, 1955). Long profiles record the interaction between uplift or base-level change, which are primarily controlled by tectonics and climate (e.g., Whipple & Tucker, 1999), and the erosive potential of flows passing through the channel, primarily controlled by sediment supply, sediment character, and discharge (e.g., Snow & Slinger- land, 1987). Therefore, long profiles have been used extensively to assess landscape evolution (e.g., Mack- in, 1948; Ouchi, 1985; Roberts & White, 2010; Sklar & Dietrich, 1998; Snyder et al., 2000).

Subaerial long profiles tend to evolve through an inverse power-law relationship between the profile slope and drainage area, that is, long profiles flatten downstream as the contributing drainage area increases. The rate at which a long profile flattens downstream is known as its concavity (e.g., Zaprowski et al., 2005), and is often used to describe the shape of a long profile (e.g., Roe et al., 2002; Sinha & Parker, 1996). Under steady state conditions, when uplift equals erosion, long profiles tend to be concave-up, whereas under nonsteady state conditions, often driven by base-level change or tectonic deformation (e.g., Whipple & Tucker, 1999), profiles tend to be less concave, or convex-up. Spatial and temporal changes in long profile concavity can, therefore, be used to assess the influence of external processes acting on the profile. Rivers flowing across active faults in Italy, for example, are more convex than those flowing over relatively inactive faults (Whittaker et al., 2008), and rivers in eastern North America become more concave with increasing precipitation (Zaprowski et al., 2005).

This concept has also been applied at a global scale, with rivers formed in arid environments found to have decreased concavity (Chen et al., 2019) and rivers formed in tectonically active environments found to have increased concavity (Seybold et al., 2021). This observation was demonstrated theoretically by Seybold et al. (2021), who derived the elevation of a long profile as a function of the uplift gradient. Using this derivation, Seybold et al. (2021) showed that more convex profiles are expected to form when tectonic uplift is focused in the upstream parts of a channel, indicating that on a global scale rivers in tectonically active environments are predominantly affected by uplift in their upstream extents.

While subaerial valleys and submarine canyons are formed by different sedimentary processes, they both evolve in superficially similar fashions, with both being subject to substrate erosion by streamflow along their thalweg and retrogressive slope failure along their margins (Mitchell, 2004, 2005). Application of geomorphic methods traditionally applied in subaerial environments to submarine environments has therefore led to insights into the processes and evolution of submarine canyons (e.g., Adams & Schlager, 2000; Am- blas et al., 2012; Brothers et al., 2013; Covault et al., 2011; Gerber et al., 2009; O'Grady et al., 2000; Pettinga & Jobe, 2020; Pirmez et al., 2000; Ramsey et al., 2006). The different impinging processes, such as background sedimentation (e.g., Gerber et al., 2009), the paucity of direct measurements, and reduced bathymetric res- olution, however, has made the controls on submarine long profile shape more difficult to constrain than those of their subaerial counterparts.

The global variability of submarine slope concavities has been studied previously by Covault et al. (2011), through the analysis of 20 present-day canyons, by Adams and Schlager (2000), through the analysis of 150 seismic profiles of submarine slopes by O'Grady et al. (2000), who categorized 50 different passive margin slopes, and Pettinga and Jobe (2020), who studied the difference between 50 submarine canyon and channel profiles and their adjacent open slope profile. Key findings from Covault et al. (2011) were that canyons formed on convergent margins and

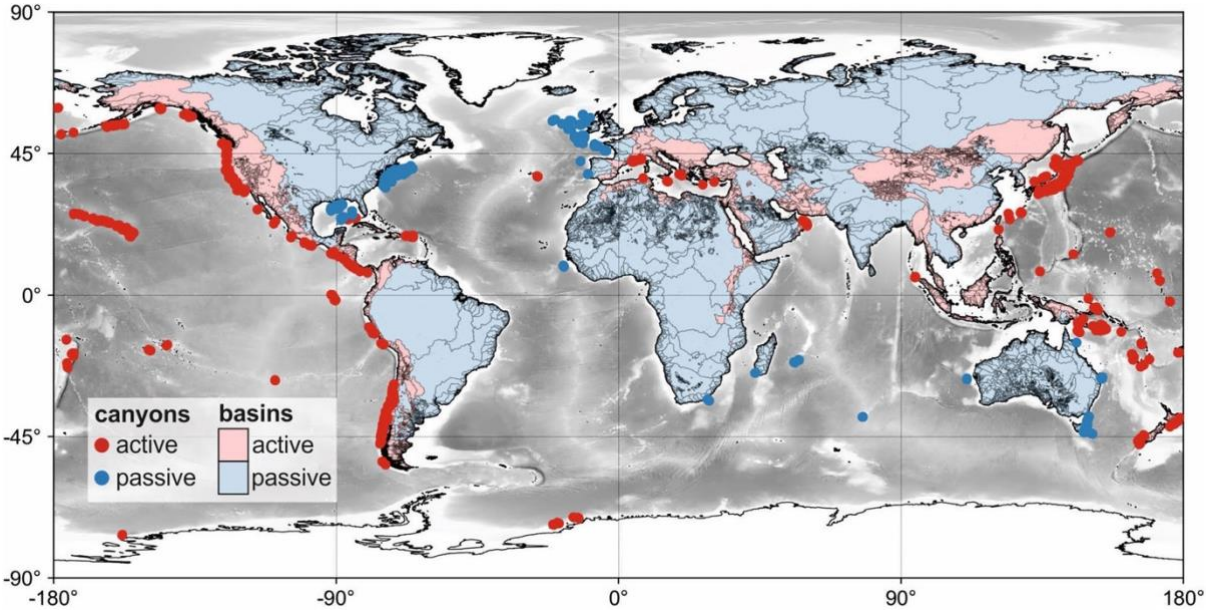

Figure 1. Submarine canyons (Harris & Whiteway, 2011), bathymetry (ETOPO1; Amante & Eakins, 2009) and drainage-basin delineation (Nyberg et al., 2018) used in this study. Red dots indicate canyons formed on active margins and blue dots indicate canyons formed on passive margins or in tectonically quiescent basins (as defined by Nyberg et al., 2018). Drainage basin delineation from (Nyberg et al., 2018). Lighter shades are shallower bathymetry, darker shades are deeper bathymetry (clipped at 4500 m).

gravitationally deforming passive margins tend to be more convex, while canyons formed on short and steep margins subject to highly erosive gravity flows tend to be more concave. Pettinga and Jobe (2020) reached similar conclusions, with tectonic deformation acting as a major influence on the morphology of submarine slopes and therefore the ability of submarine conduits to reach equilibrium, or "grade."

Based on this previous work, we therefore seek to test the hypotheses that; (1) tectonically active margins have less concave profiles, and (2) short, steep margins subject to high rates of sediment supply have more concave profiles. We test these hypotheses by measuring the concavity of 377 long profiles extracted from an existing map of present-day submarine canyons (Figure 1; Harris & Whiteway, 2011). Climatic, oceano- graphic, and tectonic datasets are also incorporated, with the aim of: (1) quantifying the global distribution of submarine canyon concavities, and (2)

quantifying the dominant controls on modern submarine canyon concavity at a global and continental-margin scale (Figure 1).

2. Methodology

2.1. Submarine Canyons

The global distribution of modern submarine canyons, and their positions, spacings, average sinuosities, dendricities (number of tributary canyons), and gradients were measured by Harris and Whiteway (2011) (Figure 1). Canyons were mapped by Harris and Whiteway (2011) through automated drainage path analysis and manual mapping of the 1 arc-minute (0.017°) ETOPO1 global bathymetric relief map (Amante & Eakins, 2009; Figure 1). The ETOPO1 map is a stitched compilation of different bathymetric data sources, such as the General Bathymetric Chart of the Oceans (GEBCO) and the US Coastal Relief Model (NGDC). The ETOPO1 map is formed by either gravity-constrained or sounding-constrained interpolation between direct measurements derived from ship-track soundings.

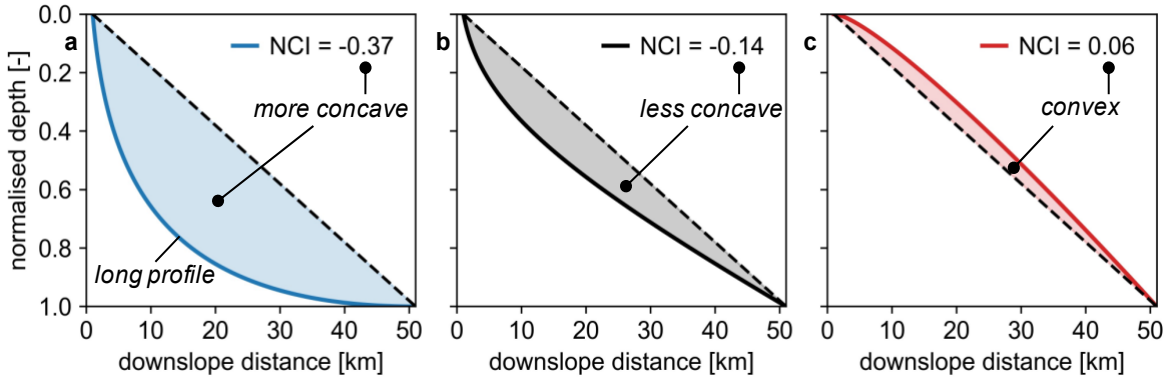

Figure 2: The long profiles of a 50 km long canyon subject to varying uplift gradients (see Seybold et al. 2021 for solution). Upstream uplift results in concave profiles with low NCI values (a), and downstream uplift results in convex profiles with high NCI values (c). Depth instead of elevation is plotted to visualise a submarine profile. Parameters are: = 1 mm yr^{-1}, x_0 = 1 km L = 50 km, k = 10 mm yr^{-1} km^{-1}, k_h =1 km $^{-0.2}$, m = 0.5, n = 1, h = 0.6.

The mapping by Harris and Whiteway (2011) required certain criteria to be met, with each canyon: (1) spanning >1,000 m depth range, (2) having a width/depth ratio less than 150:1, (3) incising greater than 100 m into the seafloor throughout their length, and (4) having a head that is shallower than 4,000 m be- low sea-level. Canyons formed on abyssal relief, such as mid-ocean ridges and seamounts ("non-margin" canyons or channels; Peakall & Sumner, 2015), were also excluded. These criteria are enforced by data resolution and therefore necessarily exclude some canyons. It is expected, however, that this consistent approach will yield representative trends. Canyon

tributaries mapped by Harris and Whiteway (2011) are not used in this study; only the main canyon profile is analyzed. Tributary data along the length of the main canyon are instead accounted for by dendricity measurements. It is important to mention that this study seeks to study canyons, as defined by Harris and Whiteway (2011), and not their associated channels. This is contrast to Covault et al. (2011) and Pettinga and Jobe (2020), who analyzed the profiles of canyons and their associated channels.

2.2. Longitudinal Profiles and the Normalized Concavity Index (NCI)

Long profiles were extracted from each canyon by sampling the depth of the canyon trace over the ETOPO1 bathymetry (Amante & Eakins, 2009), on which the canyons were originally mapped (Figures 2–4). Canyon traces were sampled at 0.01° (~1 km) intervals on a WGS-84 projection, with the metric distance between each point measured using Vincenty's geodetic formulas (Vincenty, 1975). This resulted in differences in measured lengths between Harris and Whiteway (2011), who used a different method, and this study (median difference of 4 km). This difference

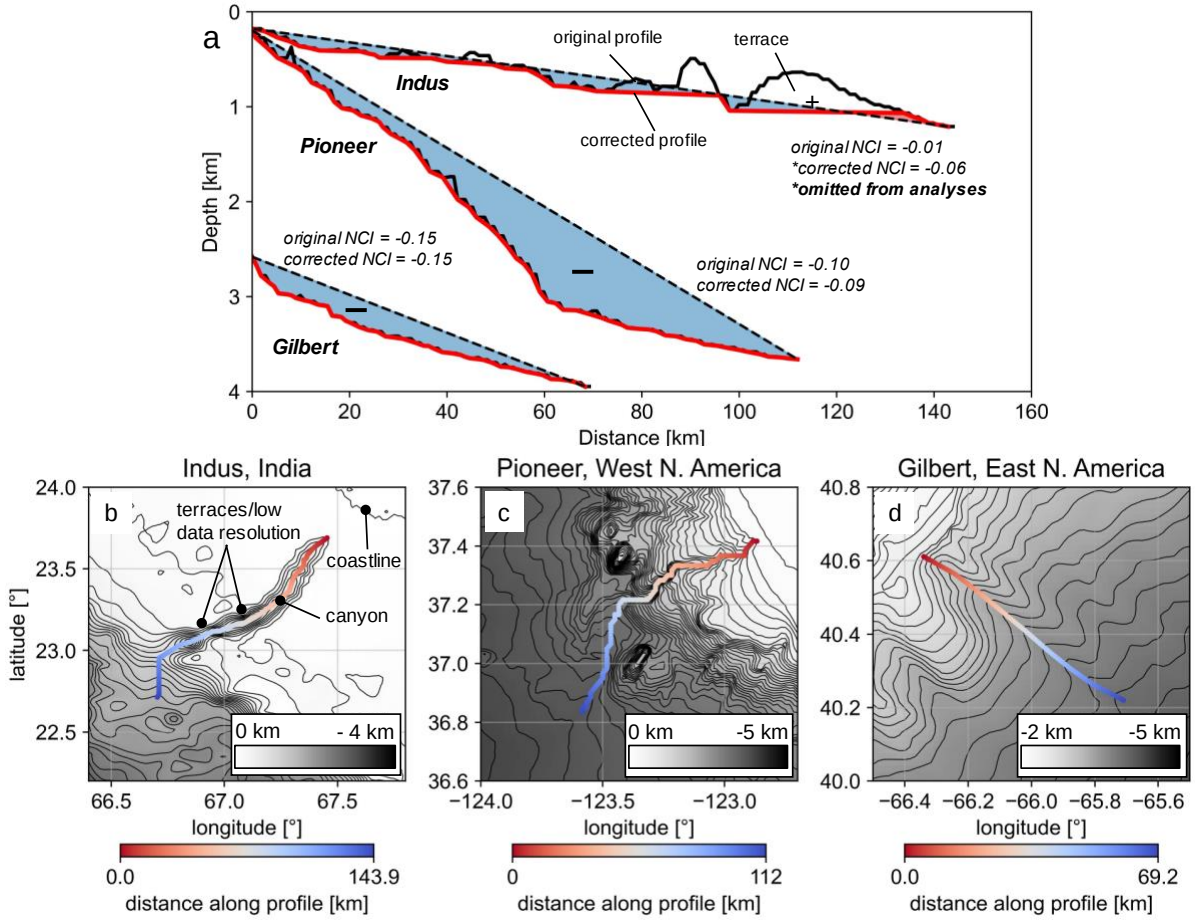

Figure 3: Three long profiles generated by this study and the correction applied to them to remove terrace deposition and irregular mapping. The original normalized concavity index (NCI) and the corrected NCI are shown. b) Indus canyon. Note that the contours squeeze where terraces or data resolution is reduced, resulting in a less certain concavity measurement. c) Pioneer canyon, d) Gilbert canyon. Contours at 500 m intervals.

155 does not affect the results because the NCI measurement is distance-normalized. In order to
156 mitigate against the potential for profile smoothing by mapping across lower-resolution sections
157 of the ETOPO1 map, only canyons where the majority of depth samples are sounding-constrained
158 were analyzed, with canyons interpolated by gravity, and Arctic canyons, omitted from the analyses
159 (Figs. S1, S3, S4).
160
161 Sediment deposition within some of the canyons, forming internal terrace and levee deposits (e.g.
162 Hansen et al., 2015), led to areas of steep positive slope within some mapped canyon profiles that
163 do not represent the thalweg (Fig. 3b). Sampling below bathymetric resolution also created areas
164 of flat slope that similarly do not represent the thalweg. A correction was applied to each profile
165 to remove flat and upstream slopes and create a continuous downstream slope, thus better
166 representing the canyon thalweg (Figure 3a). If the correction resulted in a concavity change of
167 greater than 0.01 (~0.2 std. dev of all the errors) then the canyon was omitted from the analysis,
168 under the assumption that the intra-canyon deposition was too severe to allow for a reliable
169 concavity measurement (Figures 3a, S1 and S2). These omissions, coupled with the soundings
170 omissions, result in 377 canyons being selected from the original 5,849 mapped by Harris and
171 Whiteway (2011) (Figure 5). The criteria used for these omissions is strict, but aims to greatly
172 improve the reliability of the results. The corrected, uncorrected and omitted profiles and
173 concavities of all 5849 canyons have also been recorded (Fig. S3; supplementary data).

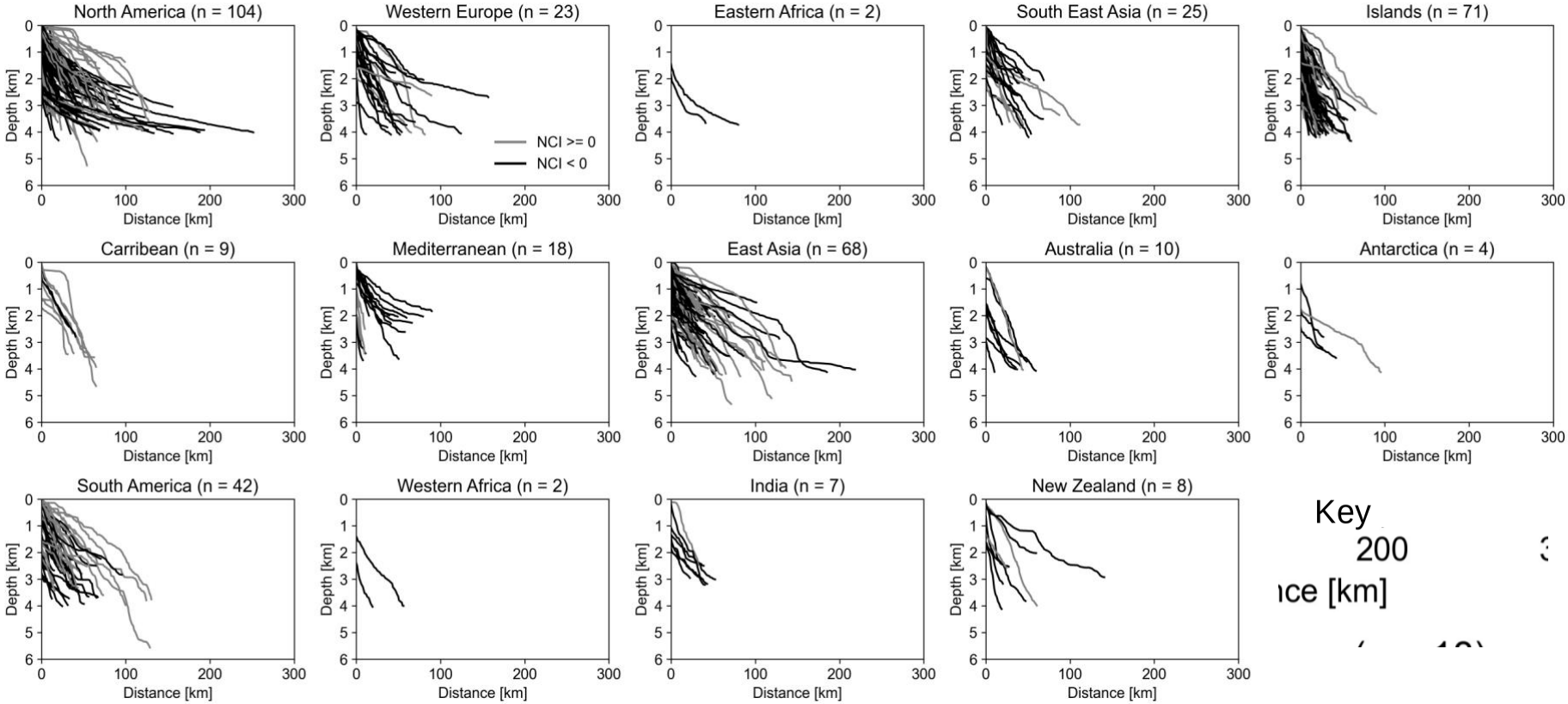

Figure 4: All long profiles generated by this study from each geographic location as defined by Harris & Whiteway (2011).

The concavity of each profile is represented by the normalized concavity index (NCI), which measures the elevation difference between a straight line fitted between the most upstream and downstream profile points, and the measured profile (Chen et al., 2019):

$$NCI = median[\frac{(E_L - Y_L)}{(E_0 - E_n)}] \quad \text{(Eq. 1)}$$

where *EL* is the depth at each point on the measured profile, *YL* is the depth at each point on the fitted straight line, *E*0 is the most upstream point of the measured profile, and *En* is the most downstream point of the measured profile. Linear profiles therefore have an NCI value of zero, while more concave profiles have more negative values, and more convex profiles have more positive values (Figures 2–5).

2.3. Underlying Controls

Following the methods used to assess the global controls on subaerial concavities (Chen et al., 2019; Seybold et al., 2021), each submarine canyon profile and its concavity was spatially merged with a number of different geomorphological, climatic and tectonic datasets (Figure 1). Canyon-specific geomorphological variables, such as sinuosity and position on the slope, are from Harris and Whiteway (2011), while more general geomorphological variables, such as onshore relief, shelf gradient, and basin type are taken from Nyberg et al. (2018). Climatic impacts on concavity were assessed by pairing each profile to the dominant climate zone of the nearest catchment (Nyberg & Howell, 2015; Nyberg et al., 2018). The fives zones (arid, equatorial, warm temperate, snow (continental), and polar) are based on the Köppen-Geiger climate zone classification (Kottek et al., 2006), which groups terrestrial climates based on seasonal precipitation and temperature ranges. Climatic impacts were also investigated by pairing each profile to the nearest drainage-basin-averaged mean annual precipitation value (Fick & Hijmans, 2017), and drainage-basin-averaged aridity index (Zomer et al., 2008).

The impact of tectonics on concavity was assessed through grouping of canyons by the basin type in which they are located (Nyberg & Howell, 2015; Nyberg et al., 2018), and pairing them with drainage-basin averaged-onshore seismicity (peak ground acceleration with 10% exceedance probability in 50 years; Giardini et al., 1999; Figure 1). An additional basin type was differentiated within the framework of Nyberg et al. (2018) to represent canyons formed on the salt-deformed north slope of the Gulf of Mexico passive margin. Canyons are grouped into the "island" basin-type when located on oceanic crust away from major continental lithospheric basins, such as

canyons formed in Hawaii or the Azores. These islands tend to be volcanically active, and are therefore grouped as tectonically active. Canyons located on islands within major continental lithospheric basins are instead grouped by that basin, such as the NW American Aleutian or Japanese Ryukyu islands formed in back-arc settings (Nyberg & Howell, 2015; Nyberg et al., 2018).

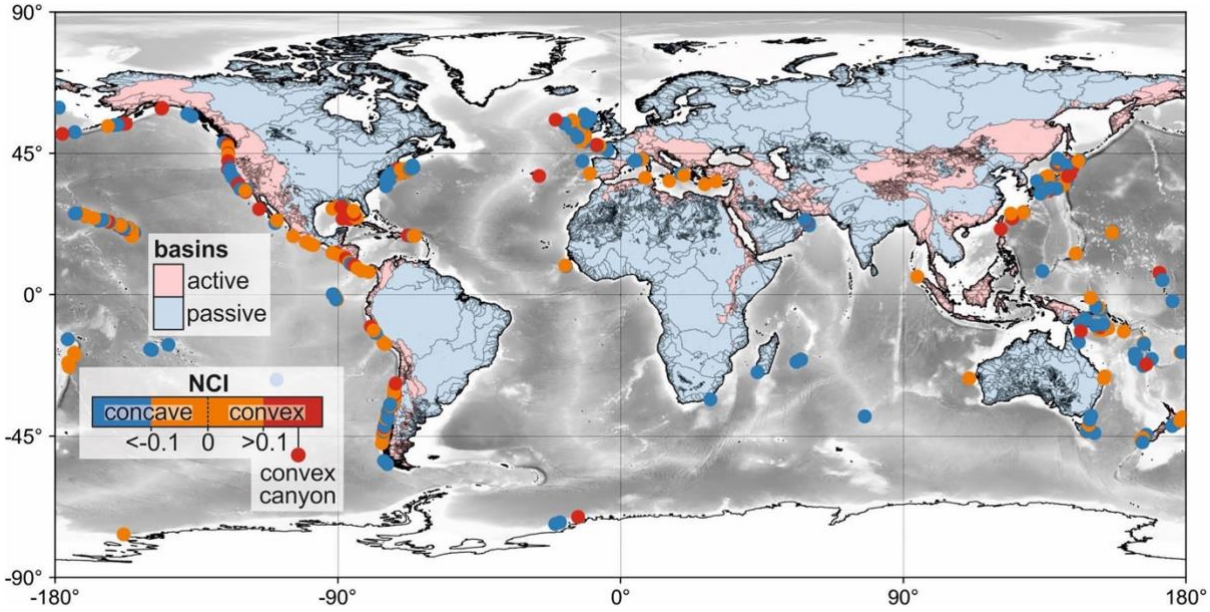

Figure 5. Submarine canyon concavities measured by this study (each canyon centered on a single point for clarity).

2.4 Statistics

Violin and kernel density estimation (KDE) plots of grouped canyon concavities were used to visually compare their differences, with the median of each distribution plotted as a straight vertical line (Fig. 6; 7). Two-sample Kolmogorov–Smirnov (KS) tests (e.g. Massey Jr, 1951) and the resulting probability values (*p*-values) were used to assess significance of differences between different distributions, with lower *p*-values indicating more significant differences. Spearman rank coefficients (ϱ) were used to assess positive or negative correlations between canyon concavity and geomorphic, tectonic and climatic variables (Fig. 8). The strength of the correlation was evaluated by the *p*-value derived from the correlation. In order to assess for correlations that may be obscured by local variation (Seybold et al., 2021), canyons were also binned and their indices averaged (median) by geographic location (e.g., western North America) and by UTM zone (Fig. 8).

3. Results

229 Detailed descriptions and interpretations of the mapped submarine canyons, such as their lengths,
230 spacings and sinuosity, are documented in Harris and Whiteway (2011). The following sections
231 will therefore focus on their longitudinal profiles.
232

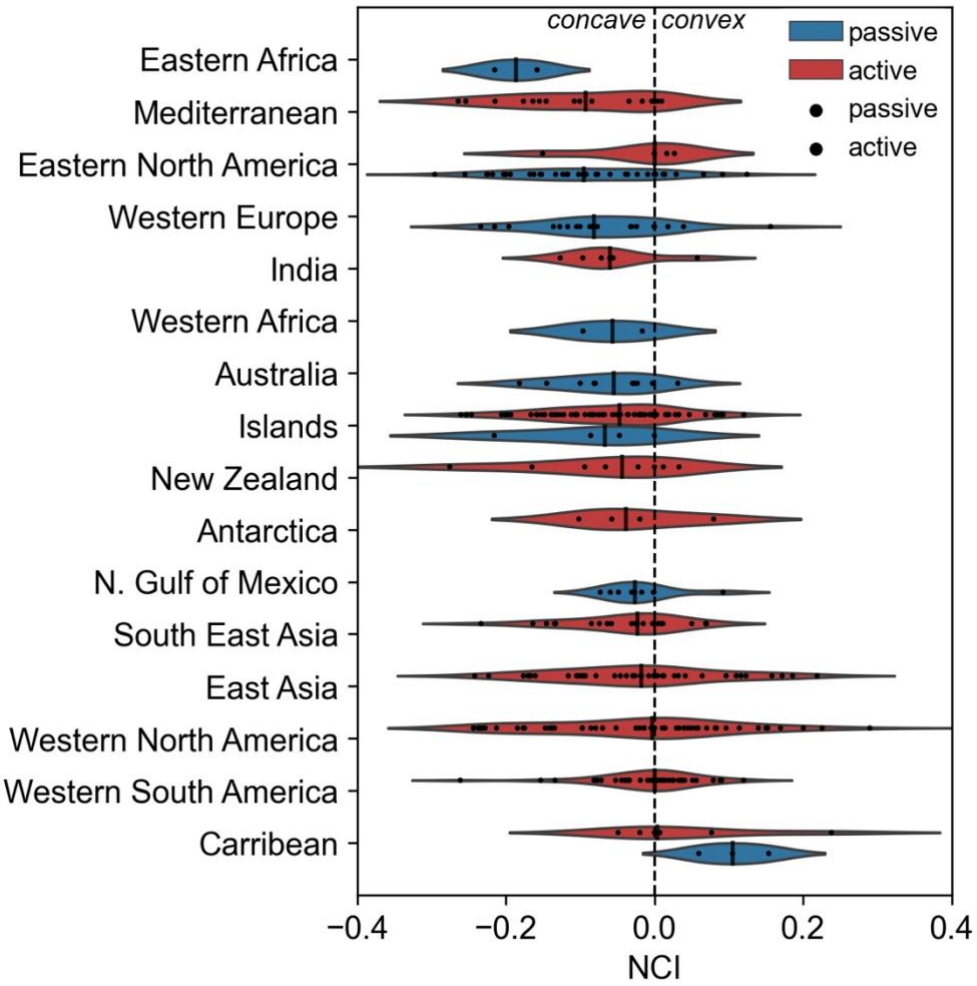

Figure 6: Violin-plot showing the distribution of NCI values for each geographic location. Geographic regions from Harris & Whiteway (2011) and active versus passive margin canyons based on Nyberg et al. (2018). Vertical black line is the median. Black dots are individual data points.

233

234 **3.1. Tectonics**

235 Longitudinal profiles were collected, and normalized concavity indices (NCI) calculated, for 5,849
236 submarine canyons (Figure S6). From this dataset, 377 canyons were filtered based on the reliability
237 of the measurement and analyzed (Figure 5). The median NCI of canyons is −0.03 and 66% of
238 canyons have NCI values less than 0, indicating that most submarine canyons are concave.
239 Submarine canyons formed on passive margins (median NCI = −0.07) are more concave than
240 those formed on active margins (me- dian NCI = −0.02; Figure 7a). Where the number of canyons
241 are greater than 10, canyons formed in the Mediterranean and the eastern North American passive

margin are the most concave, and canyons formed on the western South American convergent margin and in the Caribbean are the least concave (Figure 5). This is highlighted when canyons are grouped by basin type, with forearc basin canyons being the least con- cave ($p < 0.001$), and foreland and passive margin canyons the most concave (Figure 7c). Canyons formed on islands, back-arc, and diapiric basins have differing concavity distributions, but their differentiation is less significant compared to all other canyons (Figure 7a).

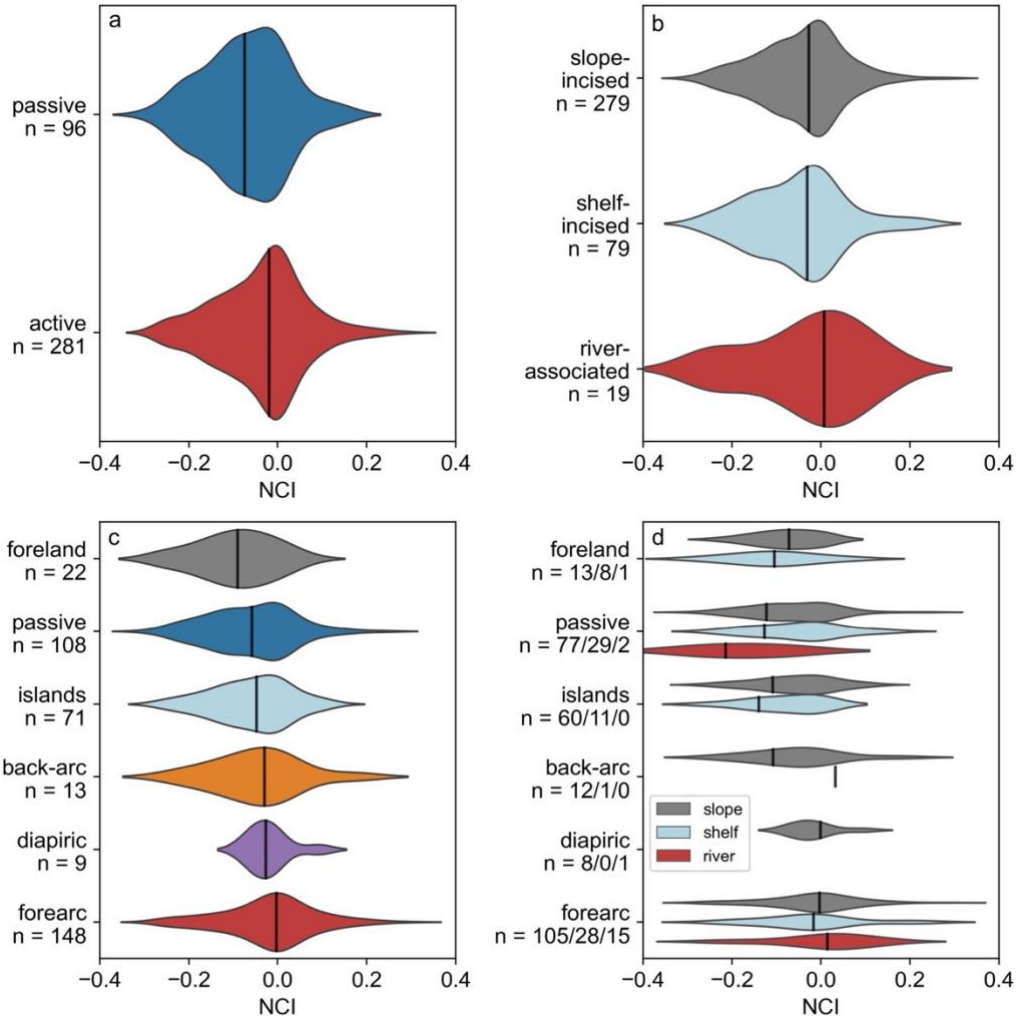

Figure 7. Violin plots showing the concavity distributions of; (a) active and passive margins, (b) slope-incised, shelf-incised and river-associated canyons, (c) canyons formed in different basins and (d) canyons formed in different positions within different basins. Margin and basin groups from Nyberg et al. (2018). Canyon positions from Harris and Whiteway (2011).

The influence of tectonics is also evident through the strong negative correlation between concavity and onshore seismicity, onshore relief and suspended sediment load (Figure 8). This is in contrast to the relationship observed within fluvial systems on a global scale (Seybold et al., 2021), where concavity increases with increasing catchment seismicity. It should be noted that

these correlations are only present when canyons are binned by geographic location, and not when taken individually or binned by UTM zone, indicating significant local variation (Figure S3).

3.2. Canyon Position

Canyon position also plays a role in adjusting concavity (Figure 7b). Slope-incised and shelf-incised sub- marine canyons, which at present day are dissociated from rivers, have less variation in concavity (std. dev. = 0.10) than shelf-incised submarine canyons with a present-day connection to a river system, termed "river-associated canyons" (std. dev. = 0.12; Harris & Whiteway, 2011). This may partly be due to the limited sample size, however. Shelf-incised and slope-incised canyons are more statistically similar (Fig- ure 7b). Where the number of river-associated, shelf-incised, and slope-incised canyons is greater than 10 for an individual basin-type (forearc basins), river association results in less concave canyons (Figure 7d). Slope-incised canyons also tend to be less concave than shelf-incised canyons within individual basin types (Figure 7d).

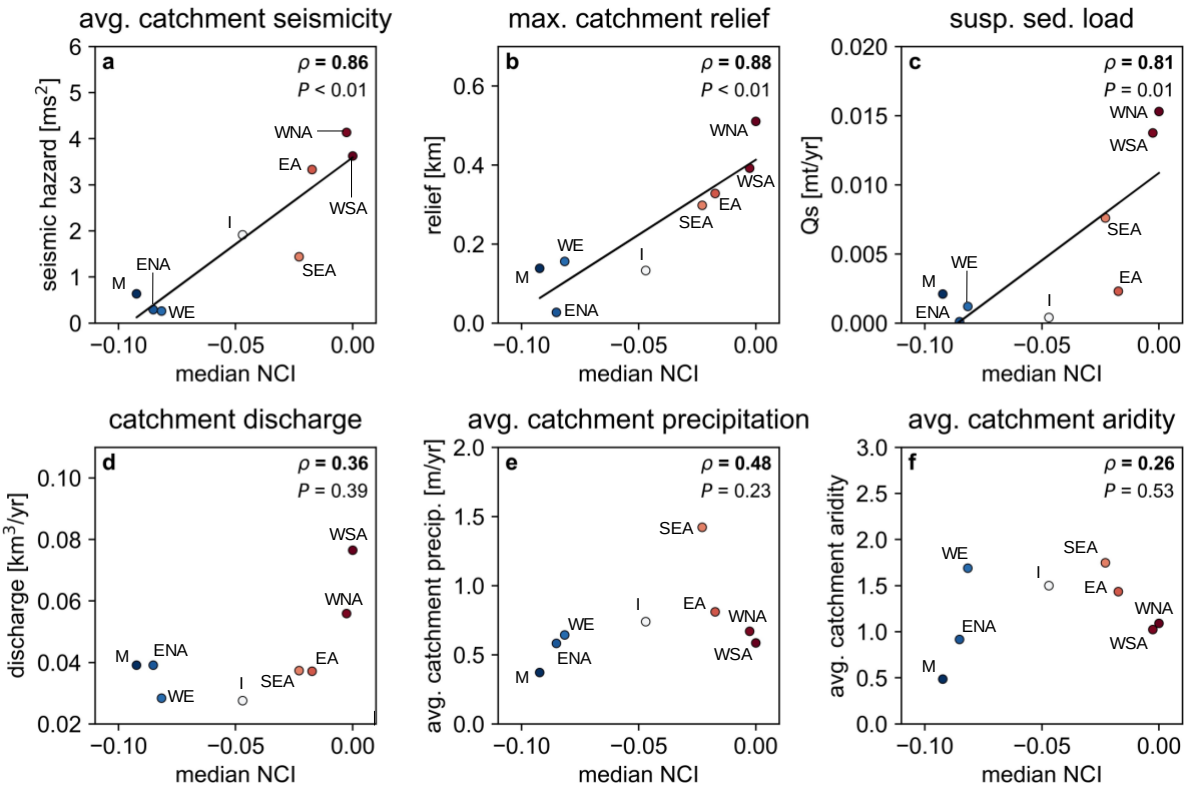

Figure 8: Correlation between canyon NCI and a) average catchment seismic risk (Giardini et al. 1999), b) maximum catchment relief (Nyberg et al. 2018), c) total suspended sediment load from catchment derived from BQART equation of Syvitski & Milliman (2007) (Nyberg et al. 2018), d) catchment discharge (Nyberg et al. 2018), e) annual average catchment precipitation (Fick & Hijmans, 2017), f) average catchment aridity (Zomer et al. 20008). Each canyon has been binned into their geographic region (e.g. Western South America) and median values taken. Spearman rank correlation (ϱ) is shown in bold, black solid line is a linear regression (only shown when $P < 0.05$). M; Mediterranean, ENA; Eastern North America, WE; Western Europe, I; Islands, SEA; South East Asia, EA; East Asia, WSA; Western South America, WNA; Western North America.

3.3. Climate

When grouped by their nearest subaerial climate regime, canyons show a wide range of different deviations that are either not statistically significant, contradictory or not maintained across groups (Figure 9). This is reflected when canyons are paired to other climatic indices, with catchment discharge, precipitation and aridity have a much weaker influence on concavities than tectonic factors (Figure 8). When river-associated canyons are isolated, a relatively strong negative correlation is documented between concavity and onshore temperature (Figure S4).

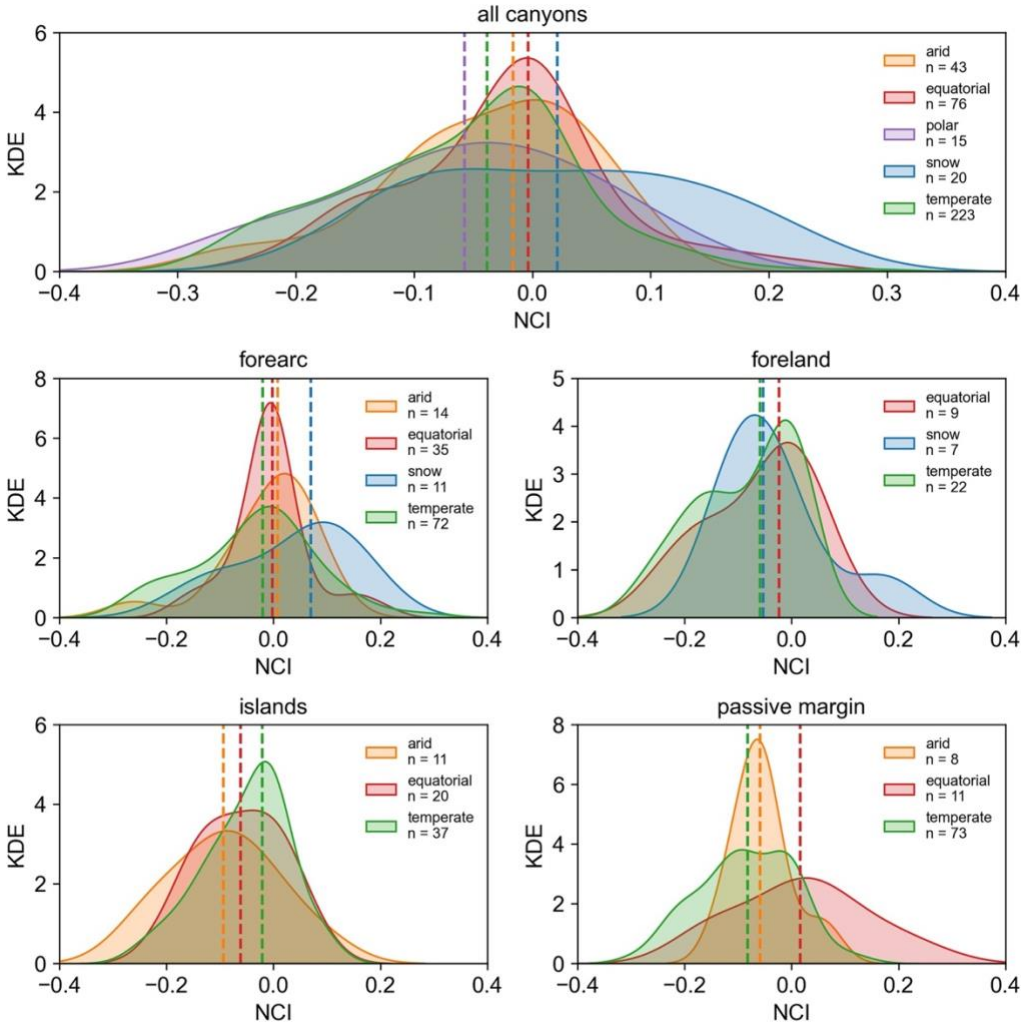

Figure 9. Kernel density estimations (KDE) of the NCI for each canyon grouped by basin type and climate zone. There is a wide variation in climate influence for each basin, indicating other factors, such as tectonics, are more important. Dashed line is the median.

3.4. Other Factors

When concavity is compared against other indices, statistically significant correlations are rare, and only observed between concavity and minimum canyon slope on a continental-margin scale (Figure 8). This relationship is not preserved on smaller scales, such as across UTM zones (Figure S4). No strong correlations are observed between other geomorphological variables, such as shelf

width, shelf gradient, and slope gradient, suggesting that these properties do not have a strong influence on submarine concavity morphology on a global or continental scale (Figure S4). When river-associated canyons are isolated, relatively strong positive correlations are documented between dendricity and concavity (Figure S4).

4. Discussion

Two ratios help to elucidate the processes controlling the concavity of submarine canyons: (1) the ratio between seafloor deformation and downslope current capacity, and (2) the ratio between sedimentation and downslope current capacity. Canyons become more concave when downslope currents have greater capacity to erode and/or transport sediment downslope, and become less concave when currents have insufficient capacity to erode or transport sediment downslope. When a profile has eroded to its equilibrium it will become bypass-dominated, with all of the sediment delivered to the canyon bypassed downslope, and no erosion or deposition occurring within the canyon itself.

4.1. Tectonism and Erodibility

When the rate of seafloor deformation exceeds the capacity of currents in the canyon to erode the substrate, canyons are expected to be less concave. This is revealed by the decreased concavity of submarine canyons formed in forearc basins (Figure 7a), which are commonly undergoing active seafloor deformation through folding, faulting or accretionary prism formation (e.g., Covault et al., 2011; Pirmez et al., 2000). The Sinú ac- cretionary prism, Colombia (Vinnels et al., 2010), and the Cook Strait, New Zealand (Micallef et al., 2014), are examples of these processes, with thrust faulting modifying the profiles of incisional submarine canyons and their channels, causing them to be convex. This trend is observed within the filtered and unfiltered datasets (Figure S6). Substrate erodibility is also expected to play a role in adjusting canyon morphology, with the low concavity values seen in Caribbean canyons partially attributed to the carbonate shelves that characterize much of the Caribbean being less erodible than siliciclastic shelves.

On passive margins, where seafloor deformation is limited to relatively few gravitationally deforming examples (e.g., Rowan et al., 2004), such as the Niger Delta (e.g., Adeogba et al., 2005; Mitchell et al., 2020), submarine canyons are generally more concave (Figure 7a), because the relatively minor or slowly deforming seafloor topography is able to be eroded by downslope currents (Figure 10a). This trend is also observed within the filtered and unfiltered datasets (Figure S6). On the diapiric Gulf of Mexico passive margin (e.g., Prather et al., 2017) concavities are similar

to those seen on convergent margins. This indicates that the rate of seafloor deformation induced by salt diapirism outpaces the rate at which flows through these canyons can erode (Figure 7c).

A strong positive correlation also exists between NCI and onshore seismicity, that is, canyons become less concave with increasing onshore seismicity (Figure 8). The opposing trend is documented in subaerial river profiles, with increasing tectonic activity resulting in a global trend toward increasing concavity as head- waters are uplifted and steepened (Seybold et al., 2021). This discrepancy may be attributed to the greater degree of uplift in the uplands of tectonically active subaerial environments compared with adjacent sub- marine environments, which is demonstrated by calculating the elevation of a long profile as a function of uplift gradient (Figure 2). When the uplift gradient is varied from upstream-focused to downstream-focused long profiles become increasingly more convex (Figure 2). This indicates that submarine canyons formed on convergent margins and adjacent to seismically active margins are subject to uplift primarily in their down-stream reaches, i.e., on the slope (Figure 10g). The high concavity values seen in canyons associated with islands may be explained by an upstream uplift gradient, with volcanic islands commonly characterized by Holocene uplift associated with isostatic rebound and magmatic underplating (e.g., Campos et al., 2010; Fretwell et al., 2010). These findings support our initial hypothesis that submarine canyons are less concave when formed on convergent or gravitationally deforming margins.

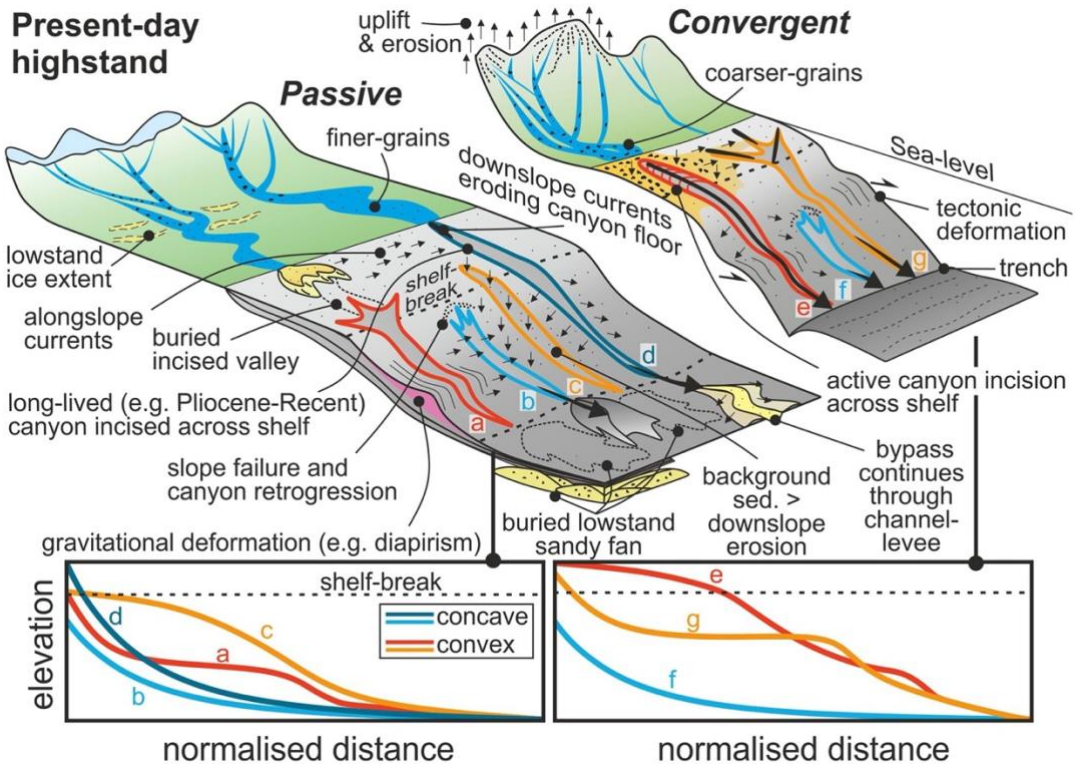

Figure 10. Schematic diagram showing the factors that may influence canyon concavity on convergent and passive margins during the present-day highstand. Passive margins have longer, low-gradient transfer zones, resulting in finer grains and less erosive flows, while convergent margins have steeper and shorter transfer zones, resulting in coarser grained, more erosive flows, and increased incision of canyons across the low-gradient shelf during highstand. Both convergent margins and passive margins may have tectonically deformed slopes, resulting in decreased concavity. Long-lived canyons with polyphase histories are also indicated as their concavity cannot be easily explained by their present-day environmental setting.

4.2. Sediment Supply and Character

When sediment supply exceeds the capacity of subaqueous currents to transport sediment downslope, or background sedimentation exceeds the rate at which subaqueous currents can erode, canyons will become less concave as the upper slope progrades sigmoidally (Amblas et al., 2012; Gerber et al., 2009; Figures 10c and 10e). This may contribute to the lower concavity values seen on canyons formed on convergent margins and canyons formed near tectonically active drainage basins, with large volumes of coarse-grained sedi- ment derived from uplifting and steep hinterlands deposited on the shelf and slope during the present-day highstand (Figure 10e). This is supported by a further decrease in concavity when forearc basins are asso- ciated with rivers (Figure 7d), which deliver vast quantities of coarse sediment to oceans in these settings (e.g., Milliman & Syvitski, 1992), and by the negative correlation between concavity and onshore seismicity, relief, and suspended sediment load (Figure 8). On active margins, however, most of this sediment tends to bypass down-slope due to the higher shelf gradients and narrower shelves

that characterize these margins (Milliman & Syvitski, 1992). This sediment may be trapped behind structures created on the slope by tectonic deformation, which can reduce the concavity of canyons formed on these margins (Covault et al., 2011). These coarse-grained flows may also modify concavity through erosion, with erosion by these flows resulting in incision of canyons across the low-gradient shelf during highstand, and therefore decreased concavity (Figure 10e). This was demonstrated on the western North American active margin, where high supplies of coarse-grained sediment increased the likelihood of canyons incising across the shelf (Smith et al., 2018). This does not support our hypothesis that submarine canyons formed on steep and narrow margins subject to high sediment supplies are likely to be more concave, and instead indicates that canyons formed on these margins are more likely to be less concave than the median in the present-day.

The impact of rivers on concavity may be reduced, or reversed, on passive margins due to the longer subaerial transport distances and finer grain-sizes delivered to most passive margins and their submarine fans (Reading & Richards, 1994; Figure 10d). Finer grains are more easily transported along and downslope by submarine currents owing to increased flow efficiency (e.g., Mutti et al., 2003), which may result in more concave profiles than those formed where the sediment supply is similar but grain sizes are larger. An exam- ple of this may be the river-associated Congo canyon on the west African passive margin, which is supplied with fine grained sediment from the Congo River (Azpiroz-Zabala et al., 2017), promoting bypass toward the Congo fan (Picot et al., 2019; Rabouille et al., 2019) and the development of a concave profile (Savoye et al., 2009). The Congo canyon is also relatively long-lived, having formed during a phase of tectonic uplift in the Pliocene that has since subsided (Ferry et al., 2004). The concavity of the Congo canyon may therefore be better explained by the environmental conditions it has been exposed to through geological time, rather than its present-day setting. This is likely the case for many individual canyons, and may be the cause of the significant local variation observed. This is difficult to constrain on a global scale, however, and requires case-by-case investigation.

Discharge and sediment supply rates are also likely to be steadier on passive margins characterized by long transfer zones, as extreme climatic and tectonic events are more easily buffered (e.g., Romans et al., 2016). This will allow sediment to be more easily bypassed downslope before it is sequestered on the shelf or in the canyon, resulting in more concave profiles. These finer-grained flows are expected to be less erosive, however, which may counteract the influence of their increased efficiency. It may therefore be more likely that the higher concavity values seen on

passive margin canyons are a consequence of their reduced ability to incise across the shelf, resulting in more of their length being preserved on the higher-gradient slope during the present day.

The influence of background sedimentation in decreasing concavity may be apparent within some stranded passive margin canyons that are relatively linear or convex, such as those seen offshore western Australia and western Europe, with erosion by the now relatively infrequent downslope currents unable to keep pace with background sedimentation and progradation along these margins (e.g., Gerber et al., 2009). Reduced concavity may also be caused by pre-existing depositional relief, formed by buried fans and channel levees, on more mature margins (Covault et al., 2011). This may also contribute to the lower concavity values observed within some passive margin canyons.

4.3. Onshore Climate

Onshore climatic effects appear to be masked by tectonics, position on the slope, or local factors in most cases (Figure 9) indicating that onshore climate plays a subsidiary role in modifying the morphology of modern submarine canyons, or that canyons are responding to onshore climate change at a slower rate than tectonics or eustasy. In this way, submarine canyons are comparable to subaerial canyons, with tectonism obscuring any potential climatic impact of fluvial geomorphology on a global scale (Seybold et al., 2021). Strong negative correlations between suspended sediment load, onshore relief and concavity are seen when the bin size is widened to a continental scale (e.g., western North America), perhaps indicating some climatic influence through enhanced run-off and sediment supply at this scale. The correlation seen between greater onshore temperatures and decreased concavity within river-associated canyons also support a relationship between climate and sedimentation, with greater chemical weathering causing enhanced sediment flux (Figure S4). These relationships may not be causal, however, as a higher sediment flux may be expected from active margins with greater relief closer to the coast through orographic precipitation and increased discharge. The influence of climate may therefore be difficult to disentangle from tectonics, as they are inextricably linked.

Climatic controls may also be difficult to assess because the climatic conditions affecting the erosional his- tory have canyons have changed through time. Latest Pleistocene-to-Holocene glacial-to-interglacial transitions and associated high fluxes of coarse-grained sediment through canyons on the NW American margin, for example, has been hypothesized to enhance the

concavities of these canyons (Covault et al., 2011). This is not easily captured using present-day global-scale indices, particularly in this study as many high-latitude canyons were omitted during data filtering.

4.4. Sea Level

Sediment bypass to deep water is known to be tied to relative sea-level changes, with rivers able to traverse the shelf and deliver sediment more easily to the shelf-edge and through submarine canyons during lowstands (e.g., Sweet et al., 2020). The present-day global highstand has therefore resulted in an abandonment of many canyons that were primarily active during the last lowstand, when sea-levels were up to 120 m lower than present (Miller et al., 2020). This will have a particular impact on long and low-gradient systems with wide shelves, such as passive margins and foreland basins (Nyberg et al., 2018), as canyons will be less able to keep pace with sea-level rise (Bernhardt & Schwanghart, 2021). This may contribute to high concavity values measured in these settings.

The incised valleys that fed these canyons during lowstand are now likely to be buried on the shelf, resulting in higher concavity values as only the steepest sections of the canyon are preserved on the slope (Figure 10a). On active margins, where incised valleys are expected to be deeper owing to steeper river gradients, canyons can be more easily traced onto the shelf as the incised valley is less likely to be fully buried during transgression and highstand (Fagherazzi et al., 2004; Harris & Whiteway, 2011; Figure 10e). Canyons formed on active margins with narrow and steep shelves are also more prone to maintaining connection with the shoreline during Holocene transgression (Bernhardt & Schwanghart, 2021). Therefore, some of the lower concavity values seen on active margin canyons may be attributed to the combination of preferential preservation of incised valley relief on the shelf and an increased ability of these canyons to incise across the shelf (Figure 10e). Again, this is in contrast to our initial hypothesis that steep and narrow margins subject to high sediment supplies tend to host more concave canyons, and instead indicates canyons formed on these margins tend to be less concave (on a global scale) owing to the increased ability of these canyons to incise across the shelf during transgression.

4.5. Slope-Incised Canyon Concavity

Most slope-incised canyons are unlikely to have been connected with rivers and direct terrigenous sediment supply even during relative sea-level falls of Quaternary magnitudes (<120 m lower), yet they are consistently concave (Figure 6c), indicating erosion and bypass of subaqueous currents. The erosive currents in these canyons must be therefore be formed by other processes, such as

retrogressive failure of the canyon head and walls (Carter et al., 2018; Sultan et al., 2007; Figures 10b and 10f).

Mechanisms for producing concave profiles in slope-incised canyons were discussed by Adams and Schlager (2000), Brothers et al. (2013), and Mitchell (2004, 2005), who hypothesized that the downstream transition from weakly erosive debris flows, derived from these canyon head and wall failures, to highly erosive turbulent flows would result in increased erosion of the canyon profile downstream and more concave long profiles. Maintenance of concave profiles in slope-incised canyons was also discussed by Jobe et al. (2011), who suggested that periodic resuspension of shelf mud and consequent plunging of thick, dilute turbidity currents erodes these canyons. This study supports these findings, further indicating that many canyons evolve predominantly through processes unrelated to direct terrigenous sediment supply.

It should also be noted that many shelf-incised canyons that were previously river-associated may now be evolving according to this process during highstand, thus increasing their concavity through time. Retrogression is likely to occur in all canyons to varying degrees, however other factors, such as terrestrial sediment input, also contributed to the evolution of shelf-incised canyons. Subaerial processes occurring during lowstand exposure of the shelf will therefore complicate the erosional history of shelf-incised canyons when compared to slope-incised canyons. Since these subaerial processes are unlikely to affect slope-incised canyons, these canyons are more likely to be affected by tectonic deformation on the slope as they are less able to smooth out any profile irregularities. Slope-incised canyons may therefore be more similar to the open slope than other canyon types, and are consequently less able to achieve grade (Pettinga & Jobe, 2020). This process is likely reflected in the higher NCI values seen on slope-incised canyons compared to shelf-incised canyons for individual basins (Figure 7d).

5. Conclusion

Modern submarine canyon longitudinal profiles and their concavities have been measured globally. The dominant control on global submarine canyon morphology is onshore tectonic activity and tectonic con- figuration, with forearc basins hosting the least concave canyons. The reduced concavity seen in forearc basins is attributed to: (1) high supply rates of coarse-grained sediment during the present-day highstand, resulting in erosion across low-gradient shelves, and (2) the rate of slope deformation being greater than the erosion rate of downslope currents. Concavity may also be decreased on passive margins by background sedimentation during highstand and through

gravitational deformation. Canyon position on the slope forms a secondary control on submarine canyon concavity, with river-associated canyons on forearcs being less concave than shelf or slope-incised canyons. This is attributed to coarse-grained sediment supplied by rivers increasing the potential for these canyons to erode across lower-gradient shelves, thus lowering the concavity of these canyons compared to shelf- and slope-incised canyons that have a greater proportion of the length stranded on the higher-gradient slope. This coarse-grained sediment may also be trapped behind tectonically-deformed structures on the slopes of these margins, resulting in less concave profiles. These factors are difficult to disentangle from climate in most cases; however, onshore climate appears to have a more limited role in modifying modern canyon morphology when compared to tectonics, indicating tectonics are the dominant influence on the concavity of submarine canyons on a global scale.

ACKNOWLEDGMENTS

Björn Nyberg, Luke Pettinga, Peter Harris, and Editor Amy East are thanked for their detailed and helpful reviews, which greatly improved the manuscript. Neil Mitchell is thanked for comments on an earlier version of the manuscript. The authors thank the Slope project Phase 5 sponsors for financial support: BP; Aker BP; BHP; CNOOC; Hess; Murphy; Neptune Energy; Vår Energi; Wintershall DEA.

DATA AVAILIBILITY STATEMENT

Datasets compiled for this study are available in the supplementary files (Tables S1 and S3) and in an on- line repository (Tables S2; https://doi.org/10.6084/m9.figshare.15172608.v1). Source data is available from Harris and Whiteway (2011) (original submarine canyon data), Nyberg et al. (2018) (geomorphological, tectonic, and climatic data), Fick and Hijmans (2017) (precipitation data), Zomer et al. (2008), (aridity index), Giardini et al. (1999) (onshore seismicity), and Amante and Eakins (2009) (bathymetry).

REFERENCES

Adams, E. W., & Schlager, W. (2000). Basic types of submarine slope curvature. *Journal of Sedimentary Research*, *70*, 814–828. https://doi. org/10.1306/2dc4093a-0e47-11d7-8643000102c1865d

514 Adeogba, A. A., McHargue, T. R., & Graham, S. A. (2005). Transient fan architecture and
515 depositional controls from near-surface 3-D seismic data, Niger Delta continental slope. *AAPG*
516 *Bulletin*, *89*, 627–643. https://doi.org/10.1306/11200404025
517
518 Amante, C., & Eakins, B. W. (2009). *ETOPO1 1 arc-minute global relief Model: Procedures, data sources*
519 *and analysis*. NOAA Technical Memorandum (p. 19). National Oceanic and Atmospheric
520 Administration.
521
522 Amblas, D., Gerber, T. P., De Mol, B., Urgeles, R., García-Castellanos, D., Canals, M., et al. (2012).
523 Survival of a submarine canyon during long-term outbuilding of a continental margin. *Geology*, *40*,
524 543–546. https://doi.org/10.1130/g33178.1
525
526 Azpiroz-Zabala, M., Cartigny, M. J., Talling, P. J., Parsons, D. R., Sumner, E. J., Clare, M. A., et al.
527 (2017). Newly recognized turbidity current structure can explain prolonged flushing of submarine
528 canyons. *Science Advances*, *3*, e1700200. https://doi.org/10.1126/sciadv.1700200
529
530 Bernhardt, A., & Schwanghart, W. (2021). Where and why do submarine canyons remain
531 connected to the shore during sea-level rise? Insights from global topographic analysis and
532 Bayesian regression. *Earth and Space Science Open Archive*.
533
534 Brothers, D. S., ten Brink, U. S., Andrews, B. D., Chaytor, J. D., & Twichell, D. C. (2013).
535 Geomorphic process fingerprints in submarine canyons. *Marine Geology*, *337*, 53–66.
536 https://doi.org/10.1016/j.margeo.2013.01.005
537
538 Campos, T. F., Bezerra, F. H., Srivastava, N. K., Vieira, M. M., & Vita-Finzi, C. (2010). Holocene
539 tectonic uplift of the St Peter and St Paul Rocks (Equatorial Atlantic) consistent with emplacement
540 by extrusion. *Marine Geology*, *271*, 177–186. https://doi.org/10.1016/j. margeo.2010.02.013
541
542 Carter, G. D., Huvenne, V. A., Gales, J. A., Iacono, C. L., Marsh, L., Ougier-Simonin, A., et al.
543 (2018). Ongoing evolution of submarine canyon rockwalls; examples from the Whittard Canyon,
544 Celtic Margin (NE Atlantic). *Progress in Oceanography*, *169*, 79–88. https://doi.
545 org/10.1016/j.pocean.2018.02.001
546

547 Chen, S. A., Michaelides, K., Grieve, S. W., & Singer, M. B. (2019). Aridity is expressed in river
548 topography globally. *Nature*, *573*, 573–577. https://doi.org/10.1038/s41586-019-1558-8
549
550 Covault, J. A., Fildani, A., Romans, B. W., & McHargue, T. (2011). The natural range of submarine
551 canyon-and-channel longitudinal pro- files. *Geosphere*, *7*, 313–332.
552 https://doi.org/10.1130/ges00610.1
553
554 Dietrich, W. E., Bellugi, D. G., Sklar, L. S., Stock, J. D., Heimsath, A. M., & Roering, J. J. (2003).
555 Geomorphic transport laws for predicting landscape form and dynamics. *Geophysical Monograph-*
556 *American Geophysical Union*, *35*, 103–132.
557
558 Fagherazzi, S., Howard, A. D., & Wiberg, P. L. (2004). Modeling fluvial erosion and deposition on
559 continental shelves during sea level cycles. *Journal of Geophysical Research*, *109*, F03010.
560 https://doi.org/10.1029/2003jf000091
561
562 Ferry, J. N., Babonneau, N., Mulder, T., Parize, O., & Raillard, S. (2004). Morphogenesis of Congo
563 submarine canyon and valley: Implica- tions about the theories of the canyons formation.
564 *Geodinamica Acta*, *17*, 241–251. https://doi.org/10.3166/ga.17.241-251
565
566 Fick, S. E., & Hijmans, R. J. (2017). WorldClim 2: New 1-km spatial resolution climate surfaces
567 for global land areas. *International Journal of Climatology*, *37*, 4302–4315.
568 https://doi.org/10.1002/joc.5086
569
570 Fretwell, P. T., Hodgson, D. A., Watcham, E. P., Bentley, M. J., & Roberts, S. J. (2010). Holocene
571 isostatic uplift of the South Shetland Islands, Antarctic Peninsula, modelled from raised beaches.
572 *Quaternary Science Reviews*, *29*, 1880–1893. https://doi.org/10.1016/j. quascirev.2010.04.006
573
574 Georgiopoulou, A., & Cartwright, J. A. (2013). A critical test of the concept of submarine
575 equilibrium profile. *Marine and Petroleum Geol- ogy*, *41*, 35–47.
576 https://doi.org/10.1016/j.marpetgeo.2012.03.003
577
578 Gerber, T. P., Amblas, D., Wolinsky, M. A., Pratson, L. F., & Canals, M. (2009). A model for the
579 long-profile shape of submarine canyons. *Journal of Geophysical Research*, *114*(F3).
580 https://doi.org/10.1029/2008jf001190

Giardini, D., Grünthal, G., Shedlock, K. M., & Zhang, P. (1999). The GSHAP global seismic hazard map. *Annals of Geophysics*, *42*, 1225– 1230. https://doi.org/10.4401/ag-3784

Hansen, L. A., Callow, R. H., Kane, I. A., Gamberi, F., Rovere, M., Cronin, B. T., & Kneller, B. C. (2015). Genesis and character of thin- bedded turbidites associated with submarine channels. *Marine and Petroleum Geology*, *67*, 852–879. https://doi.org/10.1016/j.marpetgeo. 2015.06.007

Harris, P. T., & Whiteway, T. (2011). Global distribution of large submarine canyons: Geomorphic differences between active and passive continental margins. *Marine Geology*, *285*, 69–86. https://doi.org/10.1016/j.margeo.2011.05.008

Huyghe, P., Foata, M., Deville, E., Mascle, G., & Group, C. W. (2004). Channel profiles through the active thrust front of the southern Bar- bados prism. *Geology*, *32*, 429–432. https://doi.org/10.1130/g20000.1

Jobe, Z. R., Lowe, D. R., & Uchytil, S. J. (2011). Two fundamentally different types of submarine canyons along the continental margin of Equatorial Guinea. *Marine and Petroleum Geology*, *28*(3), 843–860. https://doi.org/10.1016/j.marpetgeo.2010.07.012

Kottek, M., Grieser, J., Beck, C., Rudolf, B., & Rubel, F. (2006). World map of the Köppen-Geiger climate classification updated. *Meteorol- ogische Zeitschrift*, *15*, 259–263. https://doi.org/10.1127/0941-2948/2006/0130

Mackin, J. H. (1948). Concept of the graded river. *GSA Bulletin*, *59*, 463–512. https://doi.org/10.1130/0016-7606(1948)59[463:cotgr]2.0.co;2 Massey, F. J., Jr (1951). The Kolmogorov-Smirnov test for goodness of fit. *Journal of the American Statistical Association*, *46*, 68–78. https://doi.org/10.1080/01621459.1951.10500769

Micallef, A., Mountjoy, J. J., Barnes, P. M., Canals, M., & Lastras, G. (2014). Geomorphic response of submarine canyons to tectonic activity: Insights from the Cook Strait canyon system, New Zealand. *Geosphere*, *10*, 905–929. https://doi.org/10.1130/ges01040.1

614 Miller, K. G., Browning, J. V., Schmelz, W. J., Kopp, R. E., Mountain, G. S., & Wright, J. D.
615 (2020). Cenozoic sea-level and cryospheric evo- lution from deep-sea geochemical and continental
616 margin records. *Science Advances*, *6*, 1346. https://doi.org/10.1126/sciadv.aaz1346
617
618 Milliman, J. D., & Syvitski, J. P. (1992). Geomorphic/tectonic control of sediment discharge to
619 the ocean: The importance of small mountainous rivers. *The Journal of Geology*, *100*, 525–544.
620 https://doi.org/10.1086/629606
621
622 Mitchell, N. C. (2004). Form of submarine erosion from confluences in Atlantic USA continental
623 slope canyons. *American Journal of Science*, *304*, 590–611. https://doi.org/10.2475/ajs.304.7.590
624
625 Mitchell, N. C. (2005). Interpreting long-profiles of canyons in the USA Atlantic continental slope.
626 *Marine Geology*, *214*, 75–99. https://doi.
627 org/10.1016/j.margeo.2004.09.005
628
629 Mitchell, W. H., Whittaker, A. C., Mayall, M., Lonergan, L., & Pizzi, M. (2020). Quantifying the
630 relationship between structural deformation and the morphology of submarine channels on the
631 Niger Delta continental slope. *Basin Research*. In press. Available online. https://
632 doi.org/10.1111/bre.12460
633
634 Mutti, E., Tinterri, R., Benevelli, G., di Biase, D., & Cavanna, G. (2003). Deltaic, mixed and
635 turbidite sedimentation of ancient foreland basins. *Marine and Petroleum Geology*, *20*, 733–755.
636 https://doi.org/10.1016/j.marpetgeo.2003.09.001
637
638 Nyberg, B., Helland-Hansen, W., Gawthorpe, R. L., Sandbakken, P., Eide, C. H., Sømme, T., et
639 al. (2018). Revisiting morphological rela- tionships of modern source-to-sink segments as a first-
640 order approach to scale ancient sedimentary systems. *Sedimentary Geology*, *373*, 111–133.
641 https://doi.org/10.1016/j.sedgeo.2018.06.007
642
643 Nyberg, B., & Howell, J. A. (2015). Is the present the key to the past? A global characterization of
644 modern sedimentary basins. *Geology*, *43*(7), 643–646. https://doi.org/10.1130/g36669.1
645

O'Grady, D. B., Syvitski, J. P., Pratson, L. F., & Sarg, J. F. (2000). Categorizing the morphologic variability of siliciclastic passive continental margins. *Geology*, *28*(3), 207–210. https://doi.org/10.1130/0091-7613(2000)

Ouchi, S. (1985). Response of alluvial rivers to slow active tectonic movement. *GSA Bulletin*, *96*, 504–515. https://doi.org/10.1130/0016-7 606(1985)

Peakall, J., & Sumner, E. J. (2015). Submarine channel flow processes and deposits: A process-product perspective. *Geomorphology*, *244*, 95–120. https://doi.org/10.1016/j.geomorph.2015.03.005

Pettinga, L. A., & Jobe, Z. R. (2020). How submarine channels (re) shape continental margins. *Journal of Sedimentary Research*, *90*, 1581– 1600. https://doi.org/10.2110/jsr.2020.72

Picot, M., Marsset, T., Droz, L., Dennielou, B., Baudin, F., Hermoso, M., et al. (2019). Monsoon control on channel avulsions in the Late Quaternary Congo Fan. *Quaternary Science Reviews*, *204*, 149–171. https://doi.org/10.1016/j.quascirev.2018.11.033

Pirmez, C., Beaubouef, R. T., Friedmann, S. J., Mohrig, D. C., & Weimer, P. (2000). Equilibrium profile and baselevel in submarine chan- nels: Examples from Late Pleistocene systems and implications for the architecture of deepwater reservoirs. In *Global Deep-Water Reservoirs: Gulf Coast Section SEPM Foundation 20th Annual Bob F. Perkins Research Conference* (pp. 782–805). https://doi.org/10.5724/ gcs.00.15.0782

Prather, B. E., O'Byrne, C., Pirmez, C., & Sylvester, Z. (2017). Sediment partitioning, continental slopes and base-of-slope systems. *Basin Research*, *29*, 394–416. https://doi.org/10.1111/bre.12190

Rabouille, C., Dennielou, B., Baudin, F., Raimonet, M., Droz, L., Khripounoff, A., et al. (2019). Carbon and silica megasink in deep-sea sediments of the Congo terminal lobes. *Quaternary Science Reviews*, *222*, 105854. https://doi.org/10.1016/j.quascirev.2019.07.036

Ramsey, L. A., Hovius, N., Lague, D., & Liu, C. S. (2006). Topographic characteristics of the submarine Taiwan orogen. *Journal of Geophys- ical Research*, *111*(F2). https://doi.org/10.1029/2005jf000314

Reading, H. G., & Richards, M. (1994). Turbidite systems in deep-water basin margins classified by grain size and feeder system. *AAPG Bulletin*, *78*, 792–822. https://doi.org/10.1306/a25fe3bf-171b-11d7-8645000102c1865d

Roberts, G. G., & White, N. (2010). Estimating uplift rate histories from river profiles using African examples. *Journal of Geophysical Re- search*, *115*(B2). https://doi.org/10.1029/2009jb006692

Roe, G. H., Montgomery, D. R., & Hallet, B. (2002). Effects of orographic precipitation variations on the concavity of steady-state river profiles. *Geology*, *30*, 143–146. https://doi.org/10.1130/0091-7613

Romans, B. W., Castelltort, S., Covault, J. A., Fildani, A., & Walsh, J. P. (2016). Environmental signal propagation in sedimentary systems across timescales. *Earth-Science Reviews*, *153*, 7–29. https://doi.org/10.1016/j.earscirev.2015.07.012

Rowan, M. G., Peel, F. J., & Vendeville, B. C. (2004). Gravity- driven fold belts on passive margin. *AAPG Memoir*, *82*, 157–182.

Savoye, B., Babonneau, N., Dennielou, B., & Bez, M. (2009). Geological overview of the Angola–Congo margin, the Congo deep-sea fan and its submarine valleys. *Deep Sea Research Part II: Topical Studies in Oceanography*, *56*, 2169–2182. https://doi.org/10.1016/j.dsr2.2009.04.001

Seybold, H., Berghuijs, W. R., Prancevic, J. P., & Kirchner, J. W. (2021). Global dominance of tectonics over climate in shaping river longi- tudinal profiles. *Nature Geoscience*, *14*, 503–507. https://doi.org/10.1038/s41561-021-00720-5

Sinha, S. K., & Parker, G. (1996). Causes of concavity in longitudinal profiles of rivers. *Water Resources Research*, *32*, 1417–1428. https:// doi.org/10.1029/95wr03819

Sklar, L., & Dietrich, W. E. (1998). River longitudinal profiles and bedrock incision models: Stream power and the influence of sediment supply. *Geophysical Monograph-American Geophysical Union*, *107*, 237–260. https://doi.org/10.1029/gm107p0237

714 Smith, M. E., Werner, S. H., Buscombe, D., Finnegan, N. J., Sumner, E. J., & Mueller, E. R. (2018).
715 Seeking the shore: Evidence for active submarine canyon head incision due to coarse sediment
716 supply and focusing of wave energy. *Geophysical Research Letters*, *45*(22), 12–403.
717 https://doi.org/10.1029/2018gl080396
718
719 Snow, R. S., & Slingerland, R. L. (1987). Mathematical modeling of graded river profiles. *The Journal*
720 *of Geology*, *95*, 15–33. https://doi. org/10.1086/629104
721
722 Snyder, N. P., Whipple, K. X., Tucker, G. E., & Merritts, D. J. (2000). Landscape response to
723 tectonic forcing: Digital elevation model analysis of stream profiles in the Mendocino triple
724 junction region, northern California. *GSA Bulletin*, *112*, 1250–1263. https://doi.
725 org/10.1130/0016-7606
726
727 Sultan, N., Gaudin, M., Berne, S., Canals, M., Urgeles, R., & Lafuerza, S. (2007). Analysis of slope
728 failures in submarine canyon heads: An example from the Gulf of Lions. *Journal of Geophysical*
729 *Research*, *112*(F1). https://doi.org/10.1029/2005jf000408
730
731 Sweet, M. L., Gaillot, G. T., Jouet, G., Rittenour, T. M., Toucanne, S., Marsset, T., & Blum, M. D.
732 (2020). Sediment routing from shelf to basin floor in the Quaternary Golo System of Eastern
733 Corsica, France, western Mediterranean Sea. *GSA Bulletin*, *132*(5–6), 1217–1234.
734 https://doi.org/10.1130/b35181.1
735
736 Syvitski, J. P., & Milliman, J. D. (2007). Geology, geography, and humans battle for dominance
737 over the delivery of fluvial sediment to the coastal ocean. *The Journal of Geology*, *115*(1), 1–19.
738 https://doi.org/10.1086/509246
739
740 Vincenty, T. (1975). Direct and inverse solutions of geodesics on the ellipsoid with application of
741 nested equations. *Survey Review*, *23*(176), 88–93. https://doi.org/10.1179/sre.1975.23.176.88
742
743 Vinnels, J. S., Butler, R. W., McCaffrey, W. D., & Paton, D. A. (2010). Depositional processes
744 across the Sinú accretionary prism, offshore Colombia. *Marine and Petroleum Geology*, *27*, 794–809.
745 https://doi.org/10.1016/j.marpetgeo.2009.12.008
746

747 Whipple, K. X., & Tucker, G. E. (1999). Dynamics of the stream-power river incision model:
748 Implications for height limits of moun- tain ranges, landscape response timescales, and research
749 needs. *Journal of Geophysical Research*, *104*(B8), 17661–17674. https://doi.
750 org/10.1029/1999jb900120
751
752 Whittaker, A. C., Attal, M., Cowie, P. A., Tucker, G. E., & Roberts, G. (2008). Decoding temporal
753 and spatial patterns of fault uplift using transient river long profiles. *Geomorphology*, *100*, 506–526.
754 https://doi.org/10.1016/j.geomorph.2008.01.018
755
756 Yatsu, E. (1955). On the longitudinal profile of the graded river. *Eos, Transactions American*
757 *Geophysical Union*, *36*, 655–663. https://doi. org/10.1029/tr036i004p00655
758
759 Zaprowski, B. J., Pazzaglia, F. J., & Evenson, E. B. (2005). Climatic influences on profile concavity
760 and river incision. *Journal of Geophysical Research*, *110*(F3). https://doi.org/10.1029/2004jf000138
761
762 Zomer, R. J., Trabucco, A., Bossio, D. A., & Verchot, L. V. (2008). Climate change mitigation: A
763 spatial analysis of global land suitabili- ty for clean development mechanism afforestation and
764 reforestation. *Agriculture, Ecosystems & Environment*, *126*, 67–80. https://doi.
765 org/10.1016/j.agee.2008.01.014
766